Hindawi Publishing Corporation
Journal of Nanomaterials
Volume 2011, Article ID 614983, 8 pages
doi:10.1155/2011/614983

Research Article

Electrocatalytic Activity for CO, MeOH, and EtOH Oxidation on the Surface of Pt-Ru Nanoparticles Supported by Metal Oxide

Kwang-Sik Sim, Sin-Mook Lim, Hai-Doo Kwen, and Seong-Ho Choi

Department of Chemistry, Hannam University, Daejeon 305-811, Republic of Korea

Correspondence should be addressed to Seong-Ho Choi, shchoi@hnu.kr

Received 15 June 2011; Accepted 14 September 2011

Academic Editor: Steve Acquah

This paper describes the electrocatalytic activity for CO, MeOH, and EtOH oxidation on the surface of Pt-Ru nanoparticles supported by metal oxide (Nb-TiO_2-H) prepared for use in a fuel cell. To prepare Nb-TiO_2-supported Pt-Ru nanoparticles, first, the Nb-TiO_2 supports were prepared by sol-gel reaction of titanium tetraisopropoxide with a small amount of the niobium ethoxide in polystyrene (PS) colloids. Second, Pt-Ru nanoparticles were then deposited by chemical reduction of the Pt^{4+} and Ru^{3+} ions onto Nb-TiO_2 supports (Pt-Ru@Nb-TiO_2-CS). Nb element was used to reduce electrical resistance to facilitate electron transport during the electrochemical reactions on a fuel cell electrode. Finally, the Pt-Ru@Nb-TiO_2-H catalysts were formed by the removal of core-polystyrene ball from Pt-Ru@TiO_2-CS at 500°C. The successfully prepared Pt-Ru electrocatalysts were confirmed via TEM, XPS, and ICP analysis. The electrocatalytic efficiency of Pt-Ru nanoparticles was evaluated via CO, MeOH, and EtOH oxidation for use in a direct methanol fuel cell (DMFC). As a result, the Pt-Ru@Nb-TiO_2-H electrodes showed high electrocatalytic activity for the electrooxidation of CO, MeOH, and EtOH.

1. Introduction

Many researcher efforts have been devoted to improving the catalytic performance of carbon supported Pt-Ru catalysts [1–3]. In a colloidal method, dispersion and adsorption of catalytic nanoparticles on the surface of carbon supports is done in the presence of protecting agents to avoid aggregation of particles. It should be noted that the protecting agent is likely to reduce the catalytic activities of catalyst particles. In another method known as the impregnation method, a metal precursor is reduced by the carbon supports dispersed in the solution [4–6]. Carbon supports should be dispersed well without interference of a protecting agent in the suspension. In previous papers [7, 8], the Pt-Ru nanoparticles were deposited on various carbon supports using γ-irradiation to use as anode catalysts in a direct methanol fuel cell (DMFC). However, the life time of the electrode was reduced, since the carbon supports were slowly oxidized in the fuel cell, as shown in

$$\begin{aligned} &C + 2H_2O \longrightarrow CO_2 + 4H^+ + 4e^-, \\ &E^0 = 0.207\,V \text{ versus NHE at } 25^\circ C. \end{aligned} \quad (1)$$

In general, the support materials should possess the following properties: (1) a high surface area for a high level of dispersion of the nanosized catalysts, (2) low electrical resistance to facilitate electron transport during the electrochemical reactions, (3) a pore structure suitable for fuel or oxidant contact and by product release, and (4) strong interaction between the catalyst nanoparticles and the supports. Oxide materials are widely used as a support in heterogeneous catalyst, since they possess those properties. They have inherently higher stability compared to carbon in oxidizing environments [9, 10]. The use of titanium dioxide support in a fuel cell operation has been of great interest due to its stability, low cost, commercial availability in water, and ease to control size and structure [11, 12]. The potential applications of hollow nanomaterials, especially TiO_2 hollow (TiO_2-H) spheres, have been explored in various areas, such as light-trapping, chemical separation, photocatalysts, biomedicine, and optical devices [13, 14]. Compared to general core-shell nanostructures, TiO_2-H spheres are exceptional for their special internal cavity, high specific surface area, high mobility, and low density [15–17]. However, to our knowledge, little work has been reported

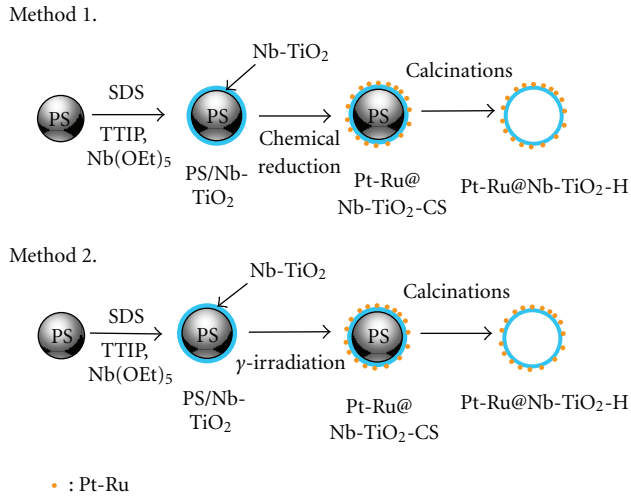

Scheme 1: Preparation procedure of the Pt-Ru@Nb-TiO_2-H catalysts by two methods.

on the application of hollow oxide spheres as a support, especially in fuel cells.

In this study, the Nb-doped TiO_2 supports were prepared with core-polystyrene and shell-Nb-TiO_2, (Nb-TiO_2-CS), for use as fuel cell anode catalysts. The Pt-Ru@Nb-TiO_2-CS was then obtained by deposition of the Pt-Ru nanoparticles on the surface of the Nb-TiO_2-CS using γ-irradiation and chemical reducing agents in aqueous solution, respectively. Finally, the Pt-Ru@Nb-TiO_2-H was fabricated via removal of the core-polystyrene from Nb-TiO_2-CS at 500°C. The electrocatalytic activity of Pt-Ru nanoparticles on metal oxide supports was evaluated via CO, methanol, and ethanol oxidation in a 0.5 M H_2SO_4 electrolyte in order to use for fuel cell anode electrode.

2. Experiment

2.1. Reagents. Styrene, sodium dodecyl sulfate (SDS), and 2-propanol (99%) were obtained from Samchun Chemical Co (Korea). Titanium tetraisopropoxide, niobium ethoxide, hydrogen hexachloroplatinate(IV) hydrate, potassium persulfate, and ruthenium(III) chloride hydrate were purchased from Sigma-Aldrich Co. (USA). Formalin and ethyl alcohol were obtained from Jin Chemical pharmaceutical Co., Ltd. (Korea). All other chemicals were in reagent grade and were used without further purification.

2.2. Synthesis of Polystyrene as Core-Ball via Surfactant-Free Emulsion Polymerization. Polystyrene nanoparticles (PS) as core-ball were prepared as follows: potassium persulfate (KPS) was dissolved completely in deionized (D.I.) water with stirring of 350 rpm for 60 min under nitrogen atmosphere. Styrene monomer was added to the above-prepared solution and polymerized at 75°C for 24 hours under nitrogen atmosphere.

2.3. Preparation of the Pt-Ru@Nb-TiO_2-H Catalysts. The Nb-TiO_2 supports were prepared by sol-gel method. SDS (0.5 g) as an anchoring agent was dissolved in the prepared PS colloids (10 mL) and stirred for 60 min under nitrogen atmosphere. Titanium tetraisopropoxide (1.2 mL) and niobium ethoxide (45 μL) were dissolved in 25 mL ethanol. The ethanol solution was slowly added to PS colloids, and the polymerization was processed while stirring (350 rpm) at 75°C for 24 hours under nitrogen atmosphere.

Scheme 1 shows the preparation procedure of Pt-Ru@Nb-TiO_2-H catalysts by chemical reduction method and γ-irradiation. In Method 1, the core-PS and shell-Nb-TiO_2 supports (0.5 g) were well dispersed in 182 mL D.I. water, and pH was adjusted to 9.0 using NaOH. Hydrogen hexachloroplatinate(IV) hydrate (0.21 g) and ruthenium(III) chloride hydrate (0.205 g) were then added to the above-prepared colloids. To reduce the Pt^{4+} and Ru^{3+} ions, the formalin, as a reducing agent, was added to the above-prepared colloids. After the Pt^{4+} and Ru^{3+} ions were reduced by ultrasonic irradiation for 60 min, the prepared Pt-Ru@Nb-TiO_2-CS nanoparticles were filtered (Whatman-2) and dried in a vacuum oven at 50°C for 8 h. Upon calcination at 500°C for 4 hrs in air, the Pt-Ru@Nb-TiO_2-H catalysts were obtained.

In Method 2, Pt-Ru@Nb-TiO_2-CS nanostructure was prepared by radiolytic reduction of Pt^{4+} and Ru^{3+} ions in the presence of the core-PS and shell-Nb-TiO_2. $H_2PtCl_6xH_2O$ (0.21 g) and $RuCl_3xH_2O$ (0.205 g) were dissolved in the Nb-TiO_2 colloids (182 mL) that contained 2-propanol (12.0 mL) as the radical scavenger. Nitrogen was bubbled for 30 min through the solution to remove oxygen, and the solution was then irradiated (Co-60 source) under atmospheric pressure and ambient temperature. A total dose of 30 kGy (a dose rate = 6.48×10^5/h) were applied. Pt-Ru@Nb-TiO_2-CS nanoparticles were filtered (Whatman-2) and dried in a vacuum oven at 50°C for 8 h. The Pt-Ru@Nb-TiO_2-H catalysts were also obtained by the method described above.

2.4. Characterization. Particle size and morphology of the Pt-Ru@Nb-TiO_2-CS and Pt-Ru@Nb-TiO_2-H catalysts were analyzed by FE-SEM (Hitachi, S-4700, Japan) and HR-TEM (JEOL, JEM-2010, USA). The content of Pt and Ru in

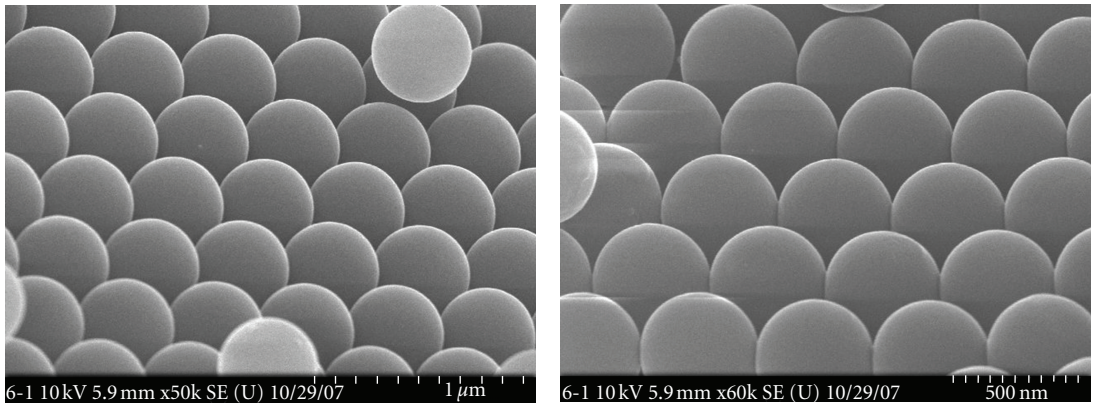

(a) (b)

Figure 1: SEM images of PS spheres as template prepared by emulsion-free polymerization.

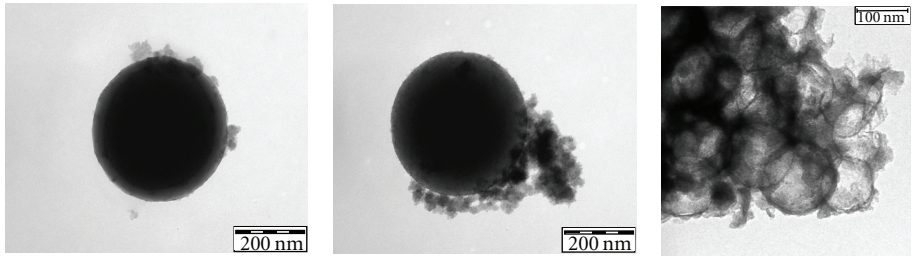

(a) (b) (c)

Figure 2: TEM images of the PS/Nb-TiO_2 (a), Pt-Ru@Nb-TiO_2-CS (b), and Pt-Ru@Nb-TiO_2 (c) prepared by Method 1 in Scheme 1.

samples was measured by inductively coupled plasma-atomic emission spectrometer (ICP-AES) (Jobin-Yvon, Ultima-C, USA). The X-ray photoelectron spectra of the samples were obtained using Thermo Fisher Scientific, MultiLab. ESCA2000, (USA). X-ray diffraction (XRD) patterns were obtained using a Japanese Rigaku D/max γA X-ray diffractometer equipped with graphite monochromatized Cu Ka radiation (λ = 0.15414 nm). The scanning range was 5–80° with a scanning rate of 5°/min.

To evaluate the catalytic efficiency of Pt-Ru@Nb-TiO_2-H catalysts for the electro-oxidation of CO, MeOH, and EtOH, the Pt-Ru@Nb-TiO_2-H catalyst electrode was prepared as follows: firstly, the catalytic inks were prepared by mixing of Pt-Ru@Nb-TiO_2-H catalysts (5.0 mg) and 5% Nafion solution (0.05 mL) and stirred for 24 h. Secondly, the catalytic inks were applied on a glass carbon (0.02 cm^2) by wet coating and dried in a vacuum oven at 50°C under nitrogen gas. The electro-oxidation of CO, MeOH, and EtOH was examined using the Pt-Ru@Nb-TiO_2-H catalyst electrode, submerged in 0.5 M H_2SO_4 electrolyte by cyclic voltammetry (EG&G INSTRUMENTS, Potentiostat/Galvanostat model 283, USA).

3. Results and Discussion

3.1. Characterization of Pt-Ru@Nb-TiO_2-H Catalysts. As mentioned above, the oxide supports for fuel cell electrode have high surface area, low electrical resistance, uniform porous structure, and interaction between catalysts and supports. In particular, surface area and electrical conductivity are very important factors in electrocatalytic reactions. The Nb-TiO_2 powder has been attractive as supports due to its high conductivity [18]. The conductivity of the Nb-TiO_2 ($\sim$0.1 Ω^{-1} cm^{-1}) is superior to that of the pure TiO_2 (10^{-6} Ω^{-1} cm^{-1}) and commercial Vulcan XC-72 carbon supports. However, the Nb-TiO_2 powder is insufficient as fuel cell supports because of low surface area. To increase surface area, the supports require nanostructure such as core-shell nanostructure or the ordered uniform porous structure.

In a previous paper [19], the PS particles of 450 nm in diameter and poly(styrene-*co*-styrene sulfonate), PSS, particles of 140–160 nm in diameter were prepared by emulsifier-free emulsion polymerization. The surfaces of the PS and PSS particles were coated with Ag nanoparticles as antimicrobial agents via reduction of Ag ions using γ-irradiation. In this study, PS particles were used as template for preparing nanostructure supports as shown in Scheme 1. Figure 1 shows SEM images of PS spheres as a template prepared by emulsion-free polymerization. The diameter of the monodispersed PS particles was 450 nm. The surface of the monodispersed PS ball possess hydrophobic properties; therefore, in order to deposit Nb-TiO_2 with hydrophilic properties, anchoring agents such as SDS, poly(N-vinylpyrrolidone), and PVP were used.

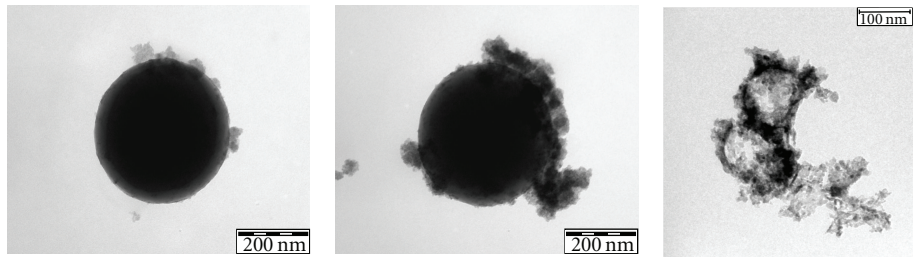

(a) (b) (c)

Figure 3: TEM images of the PS/Nb-TiO_2 (a), Pt-Ru@Nb-TiO_2-CS (b), and Pt-Ru@Nb-TiO_2 (c) prepared by Method 2 in Scheme 1.

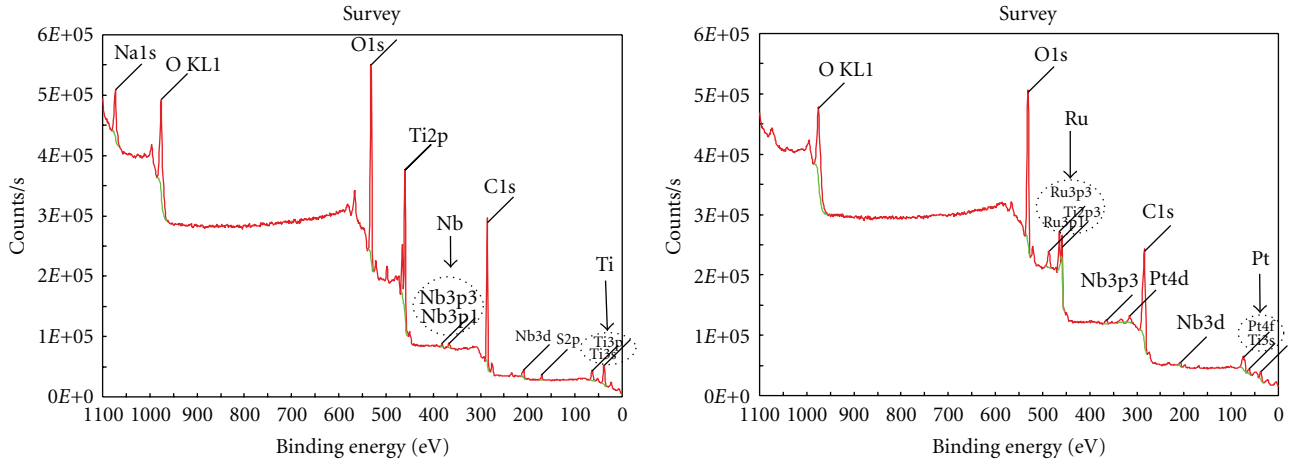

Figure 4: X-ray photoelectron spectroscopy (XPS) spectra of the PS/Nb-TiO_2 (a) and Pt-Ru@Nb-TiO_2-H (b) prepared by Method 1 in Scheme 1.

Figure 2 shows TEM images of the sphere with core-PS and shell-Nb-TiO_2, PS/Nb-TiO_2 (a), Pt-Ru@Nb-TiO_2-CS (b), and Pt-Ru@Nb-TiO_2-H (c) prepared by chemical reduction, as shown in Scheme 1. In Figure 2(a), Nb metals were deposited on the surface of TiO_2 shell wall. As shown in Figures 2(b) and 2(c), the Pt-Ru nanoparticles do not completely appear in TEM images. On the other hand, the nanostructure form (hollow form) with thickness of ~15 nm was successfully prepared as shown in Figure 2(c). Figure 3 also shows the TEM images of PS/Nb-TiO_2 (a), Pt-Ru@Nb-TiO_2-CS (b), and Pt-Ru@Nb-TiO_2-H (c) prepared by γ-irradiation as shown in Scheme 1. In Figure 3(b), after deposition of Pt-Ru nanoparticle on the surface of Nb-TiO_2 supports using γ-irradiation, the Pt-Ru nanoparticles were well dispersed on the surface of Nb-TiO_2. However, the Pt-Ru nanoparticles do not appear in TEM image. After calcinations, the patterns of Pt-Ru@Nb-TiO_2-H catalysts are different compared to that of Pt-Ru@Nb-TiO_2-H catalysts prepared by chemical reduction. This might be caused by the radiation damage of TiO_2 shell.

As mentioned above, the Pt-Ru nanoparticles cannot clearly be determined by TEM images. For clear evaluation of the existence of Pt-Ru nanoparticles, the core-PS and shell-Nb-TiO_2 supports, PS/Nb-TiO_2, and Pt-Ru@Nb-TiO_2-H were analyzed via XPS spectroscopy. Figure 4 shows the XPS data of the PS/Nb-TiO_2 (a) and Pt-Ru@Nb-TiO_2-H catalysts (b) prepared by chemical reduction. The peaks Nb and Ti element are assigned, as shown in Figure 4(a), and the Pt and Ru elements of the Pt-Ru@Nb-TiO_2-H prepared by chemical reduction were determined, as shown in Figure 4(b). These results clearly indicate that the Pt-Ru nanoparticles were successfully deposited on the surface of PS/Nb-TiO_2 by chemical reduction method. Figure 5 also shows the XPS spectra of the PS/Nb-TiO_2 nanostructure (a) and Pt-Ru@Nb-TiO_2-H catalysts (b) prepared by γ-irradiation method. The peaks Nb and Ti element are also assigned in Figure 5(a), and the Pt and Ru elements of the Pt-Ru@Nb-TiO_2-H prepared by γ-irradiation were also determined in Figure 5(b). From these results, Pt-Ru nanoparticles were successfully loaded on the surface of PS/Nb-TiO_2 nanostructure by γ-irradiation.

Figure 6 presents XRD patterns of the Pt-Ru@Nb-TiO_2-H catalysts prepared by Method 1 (a) and by Method 2 (b). Figure 6(a) shows the crystallinity of the Pt-Ru nanoparticles, and peaks are present at 39.9°, 46.2°, and 67.4°. These peaks are assigned to Pt- (111), -(200), and -(220), respectively. The (*) mark represents XRD patterns of Nb-TiO_2 nanosized supports. This means that Nb-TiO_2 supports were interpreted dominant rutile crystal structure of TiO_2. On the other hand, in Figure 6(b), the peaks of Pt-Ru nanoparticles

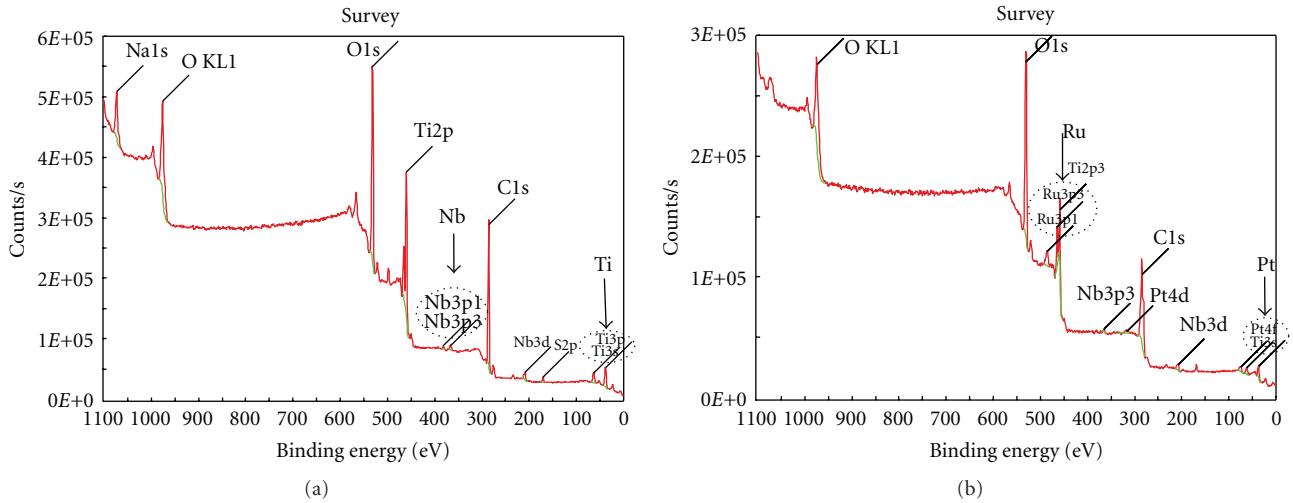

Figure 5: X-ray photoelectron spectroscopy (XPS) spectra of the PS/Nb-TiO_2 (a) and Pt-Ru@Nb-TiO_2-H (b) prepared by method 2.

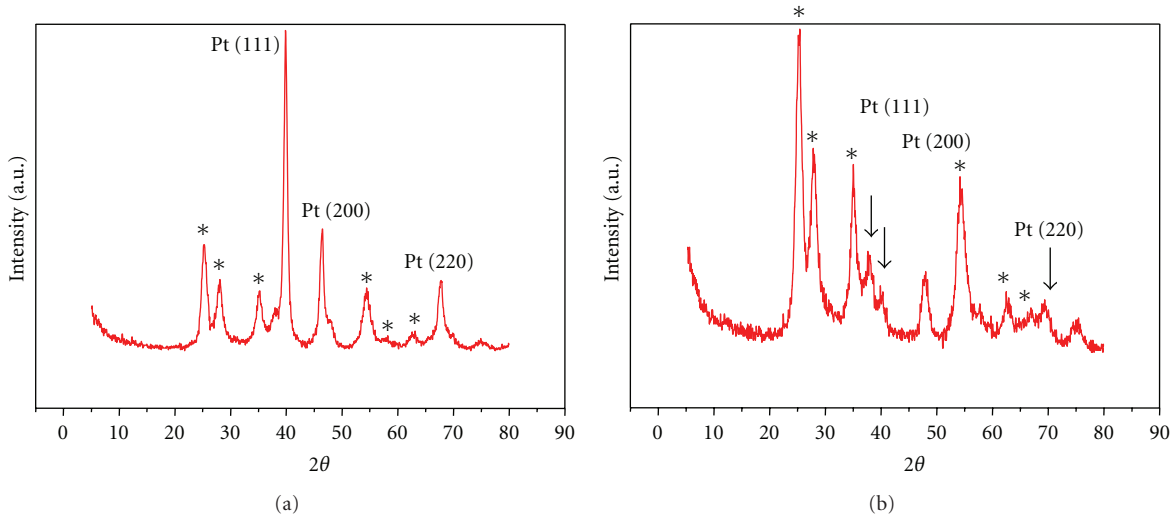

Figure 6: X-ray diffraction patterns of Pt-Ru@Nb-TiO_2-H catalyst prepared by Method 1 (a) and by Method 2 (b). The (*) markd represents XRD patterns of Nb-TiO_2 nanosized support.

on Pt-Ru@Nb-TiO_2-H catalysts shows very broad patterns compared to that of Pt-Ru nanoparticle on Pt-Ru@Nb-TiO_2-H catalysts prepared by chemical reduction. The size of Pt-Ru nanoparticle was very small compared to that of Pt-Ru@Nb-TiO_2 catalyst prepared by chemical reduction.

Table 1 presents the contents (wt-%) of Pt and Ru element in the Pt-Ru@Nb-TiO_2-H catalysts prepared by chemical reduction and γ-irradiation. When Pt-Ru alloy nanoparticles are deposited on Nb-TiO_2 supports, γ-irradiation generates slightly higher Pt content than that of Ru content, while chemical reduction produces significantly higher Ru content than that of Pt content. This may be due to the difference in the reduction potential of the two metal ions. The reduction potential of Pt ion, $[(PtCl)_4{}^{2-}\,(aq) + 2e^- \rightarrow Pt(s) + 4Cl^-\,(aq), E^0 = 0.73\,V]$, is higher than that of Ru ion. In chemical reduction, a metal ion is reduced by accepting an electron from a reducing agent. On the other hand, when the

Table 1: Contents of the containing elements in Pt-Ru@Nb-TiO_2-H prepared by Method 1 and 2 analyzed by ICP.

Sample name	Contents (wt-%)			
	Nb	Pt	Ru	Tio_2
Pt-Ru@Nb-TiO_2-H (Method 1)	2.80	0.98	6.44	40.6
Pt-Ru@Nb-TiO_2-H (Method 2)	2.78	14.4	9.40	39.4

Pt-Ru alloy nanoparticle is deposited on Nb-TiO_2 support by γ-irradiation irradiation, the hydrated electron ($e_{aq}{}^-$) is generated in aqueous solution. This hydrated electron may hold lower reduction potential, so the Pt ions are quickly reduced to that of Ru ions. The hydrated electron

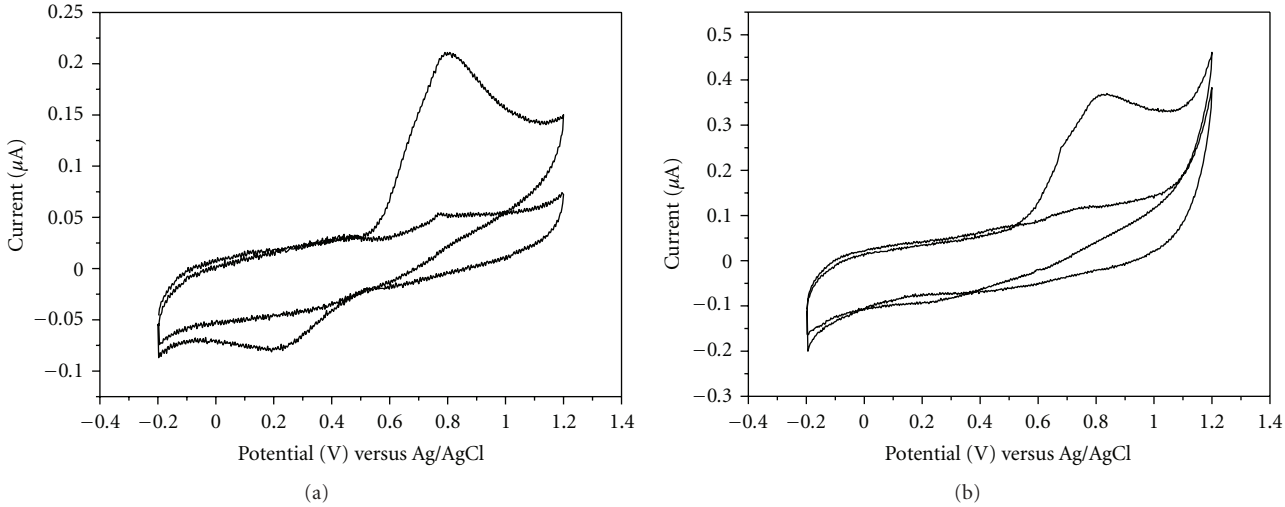

FIGURE 7: CO stripping voltammograms recorded in 0.5 M H_2SO_4 for Pt-Ru@Nb-TiO_2-H catalyst prepared by Method 1 (a) and Method 2 (b).

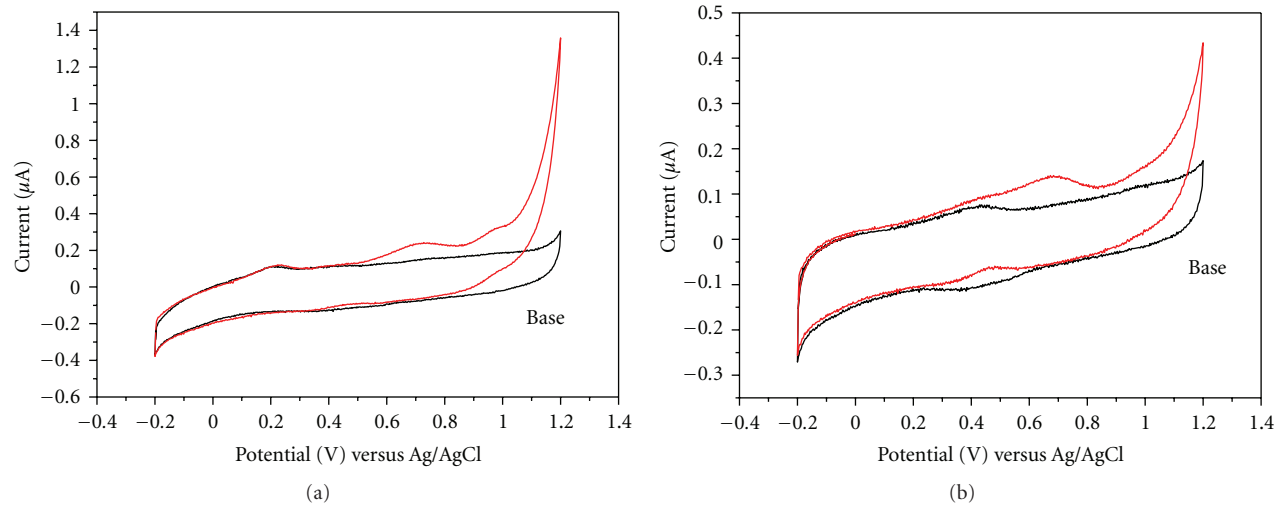

FIGURE 8: CV curves recorded in 0.5 M H_2SO_4 to 1.0 M MeOH oxidation for Pt-Ru@Nb-TiO_2-H catalysts prepared by Method 1 (a) and Method 2 (b).

produced in aqueous solution affects the yield of Pt-Ru alloy nanoparticles.

3.2. Electrocatalytic Efficiency of CO, MeOH, and EtOH Oxidation on the Surface of Pt-Ru Nanoparticles on Nb-TiO_2-H Supports. The efficiency of these catalysts toward the electrochemical oxidation of carbon monoxide (CO) was tested. Figure 7 presents the cyclic voltammograms (CVs) of electro-oxidation of CO oxidation on the Pt-Ru@Nb-TiO_2-H catalyst electrodes. Peak of stripping CO could be seen at 0.8 V for the Pt-Ru@Nb-TiO_2-H catalyst electrodes prepared by chemical reduction (a) and γ-irradiation (b). These peaks signify that CO oxidation is energetically favorable at these electrodes. The electrochemically active specific area (SEAS) of the catalysts was calculated by using the charges deduced from the CV of CO adsorption and desorption electro-oxidation process, and using the following equation [7]

$$\text{SEAS} = \frac{Q_{CO}}{G} \times 420, \tag{2}$$

where Q_{CO} is the charge for CO desorption electro-oxidation in microcolumb (μC), G represents the summation of Pt + Ru metal loading (μg) on the electrode, and 420 is the charge required to oxidize a monolayer of CO on the catalysts in $\mu C\,cm^{-2}$. The electrochemical SEASs are 58 and $36\,m^2\,g^{-1}$ for the Pt-Ru@Nb-TiO_2-H catalyst prepared by chemical reduction (a) and γ-irradiation (b), respectively. It may be considered that the higher SEAS for Pt-Ru@Nb-TiO_2-H catalyst is obtained due to the smaller particle size, even distribution, and the large loading of Pt-Ru alloy nanoparticles on the surface of Nb-TiO_2 supports.

Figure 8 presents the CVs recorded at the Pt-Ru@Nb-TiO_2-H catalyst electrodes for electro-oxidation of methanol

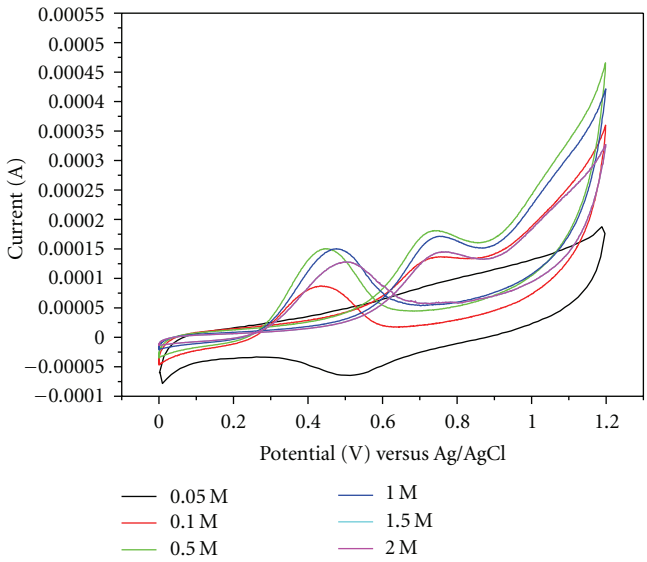

Figure 9: CV curves recorded in 0.5 M H_2SO_4 to EtOH oxidation for Pt-Ru@Nb-TiO_2-H catalysts.

in 0.5 M H_2SO_4. The peak current values at 0.7 V (versus Ag/AgCl) corresponding to the oxidation of methanol shows variation between the catalysts prepared by different routes. A larger peak current was noticed at 0.7 V (versus Ag/AgCl) for the Pt-Ru@Nb-TiO_2-H catalyst prepared by γ-irradiation (Figure 8(b)). We conclude that a higher content of Pt(wt%) in Pt-Ru@Nb-TiO_2-H catalysts (γ-irradiation) determines the catalytic efficiency towards methanol oxidation. However, as one can see in Figure 3(c), the TiO_2 supports was destroyed during γ-irradiation. Therefore, the chemical reduction assisted with ultrasonic irradiation for the deposition of Pt-Ru nanoparticles onto Nb-TiO_2 supports was better than that of γ-irradiation method as stability of metal oxide supports.

Figure 9 shows the CVs for EtOH oxidation with various concentrations onto the surface of Pt-Ru nanoparticles deposited with Nb-TiO_2 supports in 0.5 M H_2SO_4 electrolyte. The peak current values at 0.8 V (versus Ag/AgCl) corresponding to the oxidation of ethanol. The maximum catalytic efficiency was appeared in 0.5 M EtOH concentration. As a result, the prepared Pt-Ru nanoparticles onto metal oxide supports can be used in fuel cell anode electrode.

4. Conclusion

This study describes the preparation of Pt-Ru@Nb-TiO_2-H catalysts by chemical reduction assisted with ultrasonic irradiation and γ-irradiation for fuel cell anode electrode. The conclusion was as follows.

(1) The Pt-Ru@Nb-TiO_2-H catalyst was successfully prepared by chemical reduction assisted with ultrasonic irradiation and γ-irradiation.

(2) The size, morphology, and composition of Pt-Ru@Nb-TiO_2-H catalysts were determined via TEM, XRD, and elemental analysis.

(3) The Pt-Ru@TiO_2-H electrodes showed the high electrocatalytic activity for electro-oxidation of CO, MeOH, and EtOH. As a result, the catalyst prepared by chemical reduction assisted with ultrasonic irradiation can be used in a fuel cell electrode.

Acknowledgments

This research was supported by the Nano R&D program through the Korea Science and Engineering Foundation funded by the Ministry of Science and Technology. In particular, the authors would like to thank the Korea Basic Science Institute (KBSI) for FETEM measurements.

References

[1] Z. Liu, L. M. Gan, L. Hong, W. Chen, and J. Y. Lee, "Carbon-supported Pt nanoparticles as catalysts for proton exchange membrane fuel cells," *Journal of Power Sources*, vol. 139, no. 1-2, pp. 73–78, 2005.

[2] G. Chai, S. B. Yoon, S. Kang et al., "Ordered uniform porous carbons as a catalyst support in a direct methanol fuel cell," *Electrochimica Acta*, vol. 50, no. 2-3, pp. 823–826, 2004.

[3] D. F. Silva, A. O. Neto, E. S. Pino, M. Linardi, and E. V. Spinacé, "PtRu/C electrocatalysts prepared using γ-irradiation," *Journal of Power Sources*, vol. 170, no. 2, pp. 303–307, 2007.

[4] W. Chen, J. Y. Lee, and Z. Liu, "Preparation of Pt and PtRu nanoparticles supported on carbon nanotubes by microwave-assisted heating polyol process," *Materials Letters*, vol. 58, no. 25, pp. 3166–3169, 2004.

[5] K. W. Park, Y. E. Sung, S. Han, Y. Yun, and T. Hyeon, "Origin of the enhanced catalytic activity of carbon nanocoil-supported PtRu alloy electrocatalysts," *Journal of Physical Chemistry B*, vol. 108, no. 3, pp. 939–944, 2004.

[6] Z. Liu, J. Y. Lee, W. Chen, M. Han, and L. M. Gan, "Physical and electrochemical characterizations of microwave-assisted polyol preparation of carbon-supported PtRu nanoparticles," *Langmuir*, vol. 20, no. 1, pp. 181–187, 2004.

[7] K.-D. Seo, S.-D. Oh, S.-H. Choi, S.-H. Kim, H. G. Park, and Y. P. Zhang, "Radiolytic loading of the Pt-Ru nanoparticles onto the porous carbons," *Colloids and Surfaces A*, vol. 313-314, pp. 393–397, 2008.

[8] H.-B. Bae, J.-H. Ryu, B.-S. Byun, S.-H. Choi, S.-H. Kim, and C.-G. Hwang, "Radiolytic deposition of Pt-Ru catalysts on the conductive polymer coated MWNT and their catalytic efficiency for CO and MeOH," *Advanced Materials Research*, vol. 47–50, pp. 1478–1481, 2008.

[9] H. Chhina, S. Campbell, and O. Kesler, "An oxidation-resistant indium tin oxide catalyst support for proton exchange membrane fuel cells," *Journal of Power Sources*, vol. 161, no. 2, pp. 893–900, 2006.

[10] N. Zheng and G. D. Stuck, "A general synthetic strategy for oxide-supported metal nanoparticle catalysts," *Journal of the American Chemical Society*, vol. 128, no. 44, pp. 14278–14280, 2006.

[11] H. Einaga and M. Harada, "Photochemical preparation of poly(N-vinyl-2-pyrrolidone)-stabilized platinum colloids and their deposition on titanium dioxide," *Langmuir*, vol. 21, no. 6, pp. 2578–2584, 2005.

[12] M. Hepel, I. Kumarihamy, and C. J. Zhong, "Nanoporous TiO_2-supported bimetallic catalysts for methanol oxidation in acidic media," *Electrochemistry Communications*, vol. 8, no. 9, pp. 1439–1444, 2006.

[13] J. H. Pan, X. W. Zhang, A. J. Du, D. D. Sun, and J. O. Leckie, "Self-etching reconstruction of hierarchically mesoporous F-TiO_2 hollow microspherical photocatalyst for concurrent membrane water purifications," *Journal of the American Chemical Society*, vol. 130, no. 34, pp. 11256–11257, 2008.

[14] H. J. Koo, Y. J. Kim, Y. H. Lee, W. I. Lee, K. Kim, and N.-G. Park, "Nano-embossed hollow spherical TiO_2 as bifunctional material for high-efficiency dye-sensitized solar cells," *Advanced Materials*, vol. 20, no. 1, pp. 195–199, 2008.

[15] S. S. K. Kamal, P. K. Sahoo, M. Premkumar et al., "Synthesis of cobalt nanoparticles by a modified polyol process using cobalt hydrazine complex," *Journal of Alloys and Compounds*, vol. 474, no. 1-2, pp. 214–218, 2009.

[16] J. G. Yu, W. Liu, and H. G. Yu, "A one-pot approach to hierarchically nanoporous titania hollow microspheres with high photocatalytic activity," *Crystal Growth and Design*, vol. 8, no. 3, pp. 930–934, 2008.

[17] Y. Wang, F. B. Su, J. Y. Lee, and X. S. Zhao, "Crystalline carbon hollow spheres, crystalline carbon-SnO_2 hollow spheres, and crystalline SnO_2 hollow spheres: synthesis and performance in reversible Li-ion storage," *Chemistry of Materials*, vol. 18, no. 5, pp. 1347–1353, 2006.

[18] J. Chen, S. R. Bare, and T. E. Mallouk, "Development of supported bifunctional electrocatalysts for unitized regenerative fuel cells," *Journal of the Electrochemical Society*, vol. 149, no. 8, pp. A1092–A1099, 2002.

[19] S.-D. Oh, B.-S. Byun, S. Lee, and S.-H. Choi, "Preparation of Ag-PS and Ag-PSS particles by γ-irradiation and their antimicrobial efficiency againstStaphylococcus aureus ATCC 6538 andKlebsiella pneumonia ATCC 4352," *Macromolecular Research*, vol. 14, no. 2, pp. 194–198, 2006.